LAWRENCE
LIVERMORE
NATIONAL
LABORATORY

Active Creation of Instrinsically Localized Vibrations in Uranium Using X-Ray and Neutron Scattering

M.E. Manley, A. Alatas, F. Trouw, W.L. Hults, B. Leu, J.W. Lynn, Y. Chen

September 4, 2007

Disclaimer

Active creation of intrinsically localized vibrations in uranium using x-ray and neutron scattering

M. E. Manley[1], A. Alatas[2], F. Trouw[3], W. L. Hults[3], B. Leu[2], J. W. Lynn[4], Y. Chen[4, 5]

[1]*Lawrence Livermore National Laboratory, Livermore, California 94551, USA*
[2]*Argonne National Laboratory, Argonne, Illinois 60439, USA*
[3]*Los Alamos National Laboratory, Los Alamos, New Mexico 87545, USA*
[4]*NIST Center for Neutron Research, National Institute of Standards and Technology, Gaithersburg, Maryland 20899, USA*
[5]*Department of Materials Science and Engineering, University of Maryland, College Park, MD 20742 USA*

In real materials, nonlinear forces cause the frequencies of vibrating atoms to depend on amplitude. As a consequence, a large-amplitude fluctuation on the scale of the atom spacing can develop a frequency that does not resonate with the normal modes, causing energy to become trapped in an intrinsically localized mode (ILM) - also called 'discrete breather' or 'lattice soliton'[1-4]. As temperature is increased, entropy is expected to stabilize increased concentrations of these random hotspots[2]. This mechanism, which spontaneously concentrates energy, has been observed in analogous systems on a larger scale[5-10], but direct sightings at the atomic scale have proved difficult[11-14]. Two challenges have hampered progress: (1) the need to separate ILMs from modes associated with crystal imperfections, and (2) complications that arise at high temperatures, including feature broadening and multiphonon processes. Here we solve both of these problems by actively creating ILMs at low temperatures in α-uranium using high-energy inelastic x-ray and neutron scattering. The ILM creation excitation occurs at energies ten times higher than conventional lattice excitations, cleanly separating it from modes associated with crystal imperfections. The discovery of this excitation not only proves the existence of ILMs in uranium but also opens up a new route for finding ILMs in other materials and, in the process, a new area for spectroscopy.

Random localized vibrations form in uranium above 450 K and manifest as an excess in the heat capacity[14]. This excess was attributed to the configurational entropy of ILMs and used to estimate that a fraction $c \approx 0.077$ of the lattice is occupied by these states at 850 K[14]. An activation free energy $\Delta F_a \approx 180$ meV follows from the standard

expression, $\Delta F_a = -k_B T \ln(c)$. This activation free energy applies equally well to ILMs or to structural point defects, which can also lead to localized vibrations[15]. However, unlike structural defects, the atomic movement that forms an ILM is itself a vibration possessing the same polarization and spatial structure as the ILM vibrational quanta, only with an energy equal to the activation energy. At low temperatures, the activation energy is expected to differ slightly from thermal activation free energy owing to temperature effects (e.g. thermal expansion), but it should be similar. Thus, if the localized vibrations in uranium are true ILMs a matching excitation should be observable at low temperatures near 180 meV, representing the creation of the ILM from the ground state and clearly distinguishing it from a defect-induced local mode. Figure 1 illustrates how these two excitations can be used to identify an ILM.

Inelastic x-ray scattering measurements were performed at energies near 180 meV on an α-uranium single crystal at room temperature using the 3IDC-C spectrometer at the Advanced Photon Source of Argonne National Laboratory. As shown in Fig. 2a, a well defined inelastic response is observed at 160.3 meV when the scattering vector is set to Q = (0, 3, 0.8) on the [0, 1, ζ] zone boundary, but no response was detected at Q = (0, 2.12, 0.56) within the zone. Similar null results were found for Q = (0, 2.41, 0.64), and Q = (0, 2.71, 0.72) within the zone. These Q positions, folded into the first Brillouin zone, are indicated by blue symbols in Fig. 2c and show that this 160.3 meV excitation is confined near the [0, 1, ζ] zone boundary. Interestingly, the 14.3 meV ILM that forms at high temperatures occurs at the same Q point, Fig. 2b, and was also found to be confined along this zone boundary[14]. Using the BT-7 triple-axis spectrometer at the NIST Center for Neutron Research we measured two more temperatures, Fig. 2b, and also found that the excitation extends along the boundary with no energy change (dispersionless). This last detail is indicated with a red line along the zone boundary in Fig. 2c. The dominant direction of Q for both of these excitations indicates that they are polarized largely along the [010] direction. Confinement along the zone boundary shows that they are excited most effectively when $1/|Q|$ (wavelength) equals the atomic spacing and indicates a mode with atoms beating against each other, out of phase. This closely matching reciprocal-space structure indicates a direct relationship between these excitations. The fact that the 160.3 meV excitation energy is also consistent with the activation-energy scale of the

process that produced the 14.3 meV ILM, provides strong evidence that the former creates the latter. The intensity of the 160.3 meV excitation is also consistent with the vibrational mechanism of ILM creation. When corrected for width, it is a little more than an order of magnitude weaker than a 12 meV phonon in uranium, as expected since intensity for vibrations is inversely proportional to energy[16]. To definitively eliminate all possible electronic origins, however, we now turn to neutron scattering, a probe that does not interact with charge.

Inelastic neutron scattering measurements were performed on polycrystalline uranium at room temperature using 250 meV incident-energy neutrons on the PHAROS time-of-flight spectrometer at the Los Alamos Neutron Science Center. Figure 3 shows the data summed over both high and low momentum transfers. Centered at zero energy is the elastic peak, negative energies indicate neutron energy gain, and positive energies indicate neutron energy loss. At high momentum transfers a weak excitation at the expected energy of ~160 meV appears in the neutron energy loss side, indicating that this energy is being deposited in the crystal. The feature is much harder to detect at low momentum transfers. This is consistent with the behavior of lattice excitations which scale as the square of momentum transfer Q^2, while magnetic excitations are cutoff at high values of Q because of a form factor[16]. For uranium in particular, the magnetic form factor cutoff is around 1 Å^{-1}, so the observation above 9.5 Å^{-1} clearly rules out a magnetic origin[17], leaving only lattice dynamics. Neutron detection of this feature alone might be dismissed as a hydrogen impurity mode, as hydrogen has a large cross section and can produce vibrations in this energy range. However, observation of the same energy excitation in the inelastic x-ray scattering data, Fig. 2a, rules out this possibility; hydrogen is essentially invisible to the x-rays when compared to uranium. We therefore conclude that this excitation is a lattice dynamical feature of uranium with energy a full order of magnitude larger than the highest phonon excitation. This energy cannot be explained in terms of conventional lattice dynamics, but it is consistent with the energy of forming ILMs in uranium. This combined with the matching reciprocal space structure leads us to conclude that we are observing the ILM formation mechanism[1-4]. It follows that 160.3 meV is the ILM activation energy while 14.3 meV is the vibrational quanta energy of the thermally activated ILM.

This approach of identifying ILMs by creating them with high-energy scattering is applicable to many diverse areas of science where evidence for ILM formation has been indicated experimentally or theoretically; ranging from complex biological materials[12] to ionic crystals[18] to quantum solids[13]. Unlike with ILM vibrational quanta excitations above bands[2] or in gaps[18], which could be mistaken for defect modes or lost within multiphonon excitations, the ILM creation excitation energy scale is well outside that of conventional lattice dynamical processes. As a result, it can be detected in polycrystalline or powder materials. Furthermore, because active creation occurs out of equilibrium, there is no need to know what temperature ILMs become thermally activated. Even in cases where the activation energy is too high for ILMs to be practically observed below the melting temperature, creation experiments may still be possible. Thus, direct evidence for the role of ILMs in the folding of biopolymer chains[19], mechanical deformation[14], nonlinear thermal transport[20], or melting[4], might be found in high-energy lattice excitations.

1. Doglov, A. S. Localization of vibrations in a nonlinear crystalline structure. *Sov. Phys. Solid State* **28**, 907 (1986).

2. Sievers, A. J. & Takeno S., Intrinsic localized modes in anharmonic crystals. *Phys. Rev. Lett.* **61**, 970 (1988).

3. Flach, S., & Willis, C. R. Discrete breathers. *Phys. Rep.* **295**, 182−264 (1998).

4. Campbell, D. K., Flach, S. & Kivshar, Y. S. Localizing energy through nonlinearity and discreteness. *Phys. Today* **57**, 43 (2004).

5. Trias, E., Mazo, J. J. and Orlando, T. P. Discrete breathers in nonlinear lattices: Experimental detection in a Josephson array. *Phys. Rev. Lett.* **84**, 741-744 (2000).

6. Binder, P., Abraimov, D., Ustinov, A. V., Flach, S. & Zolotaryuk, Y. Observation of breathers in Josephson ladders. *Phys. Rev. Lett.* **84**, 745-748 (2000).

7. Eisenberg, H. S., Silberberg, Y. Morandotti, R., Boyd, A. R. & Aitchison, J. S. Discrete spatial optical solitons in waveguide arrays. *Phys. Rev. Lett.* **81**, 3383-3386 (1998).

8. Fleischer, J. W., Segev, M., Efremidis, N. K. & Christodoulides, D. N. Observation of two-dimensional discrete solitons in optically induced nonlinear photonic lattices. *Nature* **422**, 147-150 (2003).

9. Sato, M. & Sievers, A. J., Direct observation of the discrete character of intrinsic localized modes in an antiferromagnet. *Nature* **432**, 486-488 (2004).

10. Sato, M., Hubbard, B. E., & Sievers, A. J. Colloquium: Nonlinear energy localization and its manipulation in micromechanical oscillator arrays. *Rev. of Mod. Phys.* **78**, 137-157 (2006).

11. Swanson, B. I., Brozik, J.A., Love, S.P., Strouse, G. F., Shreve, A. P., Bishop, A. R., Wang, W.-Z., & Salkola, M. I. Observation of intrinsically localized modes in a discrete low dimensional material. *Phys. Rev. Lett.* **82**, 3288-3291 (1999).

12. Xie, A., van der Meer, L., Hoff, W. & Austin, R. H. Long-lived amide I vibrational modes in myoglobin. *Phys. Rev. Lett.* **84**, 5435-5438 (2000).

13. Markovich, T., Polturak, E., Bossy, J. & Farhi, E. Observation of a new excitation in bcc He-4 by inelastic neutron scattering, *Phys. Rev. Lett.* **88**, 195301 (2002).

14. Manley, M. E., Yethiraj, M., Sinn, H., Volz, H. M., Alatas, A., Lashley J. C., Hults, W. L., Lander, G. H., & Smith J. L. Formation of a new dynamical mode in α-uranium observed by inelastic neutron and x-ray scattering, *Phys. Rev. Lett.* **96**, 125501 (2006).

15. Maradudin, A. A., Montroll, E. W. & Weiss, G. H., *Theory of Lattice Dynamics in the Harmonic Approximation* (Academic, New York 1963).

16. Squires, G. L., *Introduction to the Theory of Neutron Scattering* (Dover, New York, 1978).

17. Freeman, A. J., Desclaux, J. P., Lander, G. H., & Faber, J. Jr. Neutron magnetic form factors of uranium ions, *Phys. Rev. B* **13**, 1168 (1976).

18. Kiselev, S. A., & Sievers, A. J., Generation of intrinsic vibrational gap modes in three-dimensional ionic crystals, *Phys. Rev. B* **55**, 5755 (1997).

19. Mingaleev, S. F., Gaididei, Yu. B., Christiansen, P. L., & Kivshar, Yu. S. Nonlinearity-induced conformational instability and dynamics of biopolymers, *Europhys. Lett.* **59**, 403 (2002).

20. Chang, C. W., Okawa, D., Majumdar, A. & Zettl A. Solid-state thermal rectifier *Science* **314**, 1121-1124 (2006).

Figure Captions:

Figure 1 Simplified intrinsically localized modes (ILMs) illustrating passive detection versus active creation. **a**, ILMs form by random thermal fluctuations and are then detected by exciting a vibrational quanta of one of the modes. **b**, an ILM is actively formed at low temperatures by imparting the energy and momentum needed to create the ILM from the ground state. The energy needed to create the ILM (activation energy) can be used to predict the temperature where the ILMs become thermally activated and both scattering events involve the same scattering geometry. Thus, a direct relationship can be established between the two types of ILM excitations.

Figure 2 Two excitations on the [01ζ] zone boundary. **a**, High-energy scattering measured on a cold (room temperature) crystal using inelastic x-ray scattering (IXS), both on and off of the zone boundary where the ILM appears. **b**, Low-energy scattering showing the ILM vibrational excitation observed forming at high temperatures using inelastic neutron scattering (INS); signals are offset for clarity. The scattering vector, Q, is in the **b-c** plane. The phonon wave vector, q, conserves momentum according to $Q = G + q$, where G is a reciprocal lattice vector pointing to the nearest reciprocal lattice point. **c**, Locations of the measured Q points folded into the first Brillioun zone. Open blue diamond symbols within the zone indicate null high-energy results (see text), while the solid symbols indicate where signals were found. The red line indicates the extension of the 14.3 meV excitation on the [01ζ] zone boundary, which was found to be dispersionless along this boundary.

Figure 3 Time-of-flight (TOF) inelastic neutron scattering (INS) spectra collected using 250 meV incident-energy neutrons on polycrystalline uranium. The top panel shows the data summed over the highest momentum transfers (Q), while the lower panel shows the data summed over the lower values of Q.
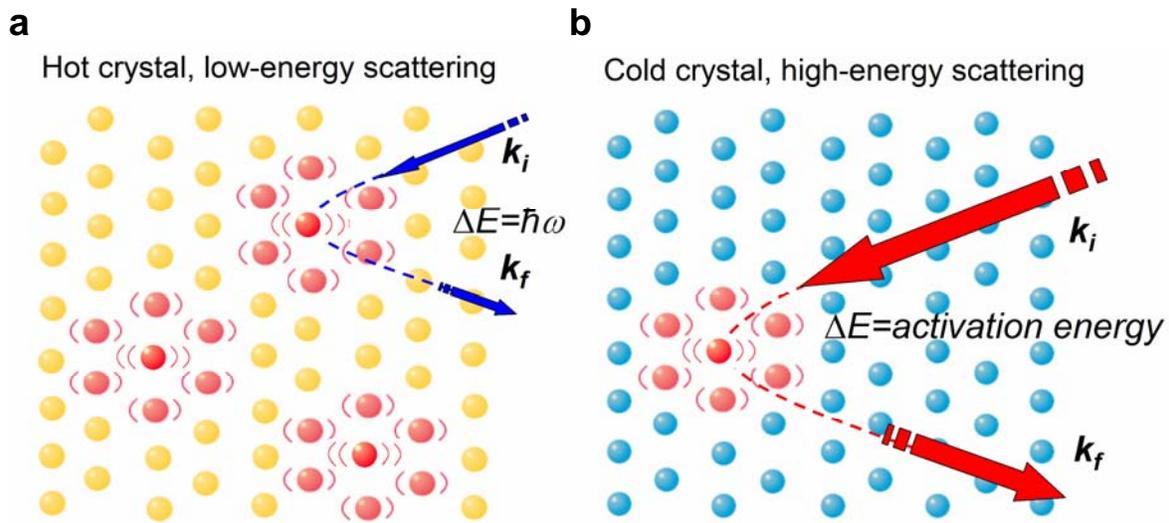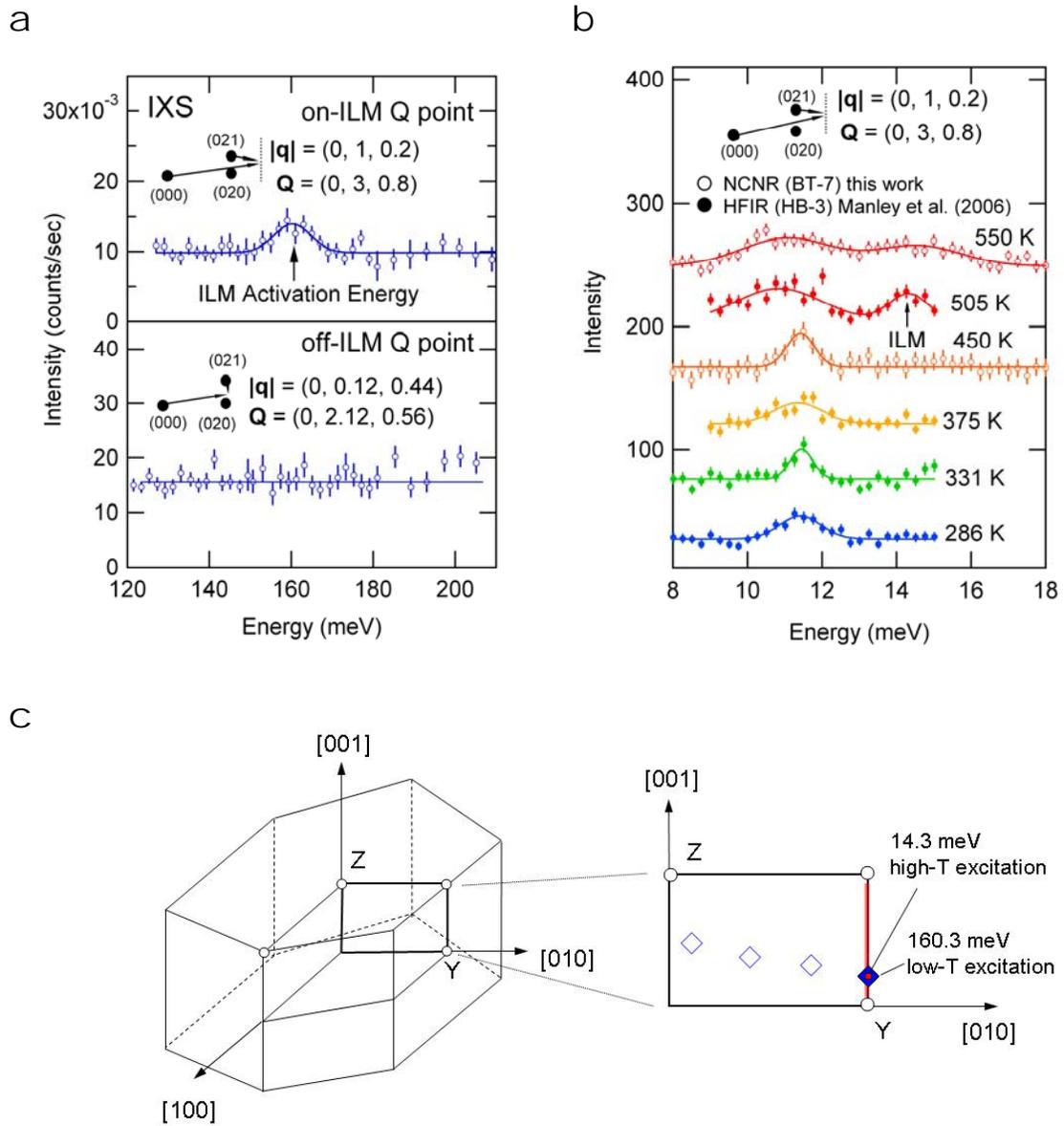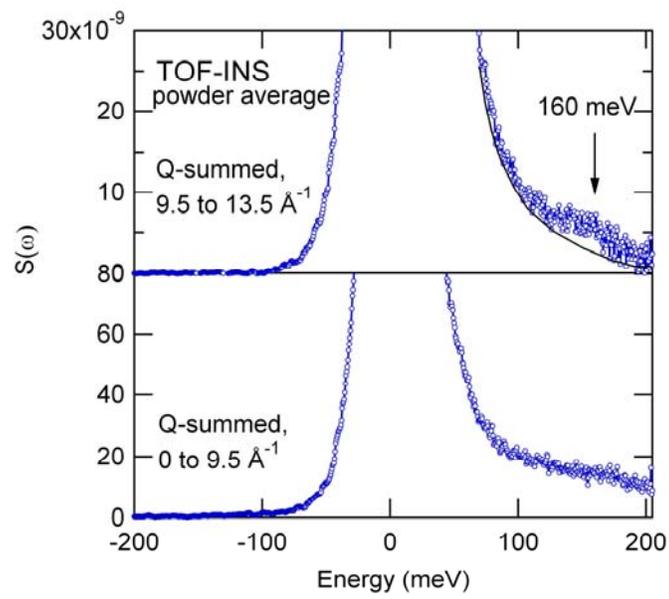
a Hot crystal, low-energy scattering

k_i

$\Delta E = \hbar \omega$

k_f

b Cold crystal, high-energy scattering

k_i

$\Delta E = activation\ energy$

k_f

Fig. 1

a

IXS

on-ILM Q point

(021)
(000) (020)

$|\mathbf{q}| = (0, 1, 0.2)$
$\mathbf{Q} = (0, 3, 0.8)$

ILM Activation Energy

off-ILM Q point

(021)
(000) (020)

$|\mathbf{q}| = (0, 0.12, 0.44)$
$\mathbf{Q} = (0, 2.12, 0.56)$

Intensity (counts/sec)

Energy (meV)

b

(021)
(000) (020)

$|\mathbf{q}| = (0, 1, 0.2)$
$\mathbf{Q} = (0, 3, 0.8)$

○ NCNR (BT-7) this work
● HFIR (HB-3) Manley et al. (2006)

550 K
505 K
ILM   450 K
375 K
331 K
286 K

Intensity

Energy (meV)

c

[001]
[010]
[100]
Z
Y

[001]
[010]
Z
Y

14.3 meV
high-T excitation

160.3 meV
low-T excitation

Fig. 2

9

Fig. 3